Proceedings of Building Simulation 2011:
12th Conference of International Building Performance Simulation Association, Sydney, 14-16 November.

NUMERICAL STUDY ON THE CARBON DIOXIDE DISTRIBUTION IN A NATURALLY VENTILATED SPACE

André Isele[1,2], Gerrit Höfker[1], Malcolm Cook[2]
[1]Institute of Building Physics, Materials and Construction,
Bochum University of Applied Science, Germany
[2]Department of Civil and Building Engineering,
Loughborough University, UK

ABSTRACT

Carbon dioxide concentration is often taken as an indicator of indoor air quality, especially in spaces where human beings are the main contaminant source. Therefore this CFD analysis focuses on the CO_2 distribution in a sports hall, representing large and high enclosures. A buoyancy driven natural ventilation system prevails in the absence of wind, so that a pollutant stratification can be expected corresponding to displacement ventilation. The results of a parametric study reveal that the most influencing factors on the vertical carbon dioxide concentration profiles in the space, in addition to the ventilation flow rate, are the thermal properties of the surrounding surfaces.

INTRODUCTION

For enclosed environments regularly accommodating a large number of people, such as classrooms and theatres, carbon dioxide is often used as the key indicator of indoor air quality in the absence of any other major pollutants. Guidelines call for the compliance with upper limiting values of the average concentration of carbon dioxide. In this context it often appears that 1500 ppm should not be exceeded in all teaching and learning spaces (Building Bulletin 101, 2006), which is also a common guideline value for other premises. However, the actual distribution of contaminants throughout a space can vary with its ventilation system.

The objective of this research, therefore, is to examine the distribution of carbon dioxide as a proxy for occupant–related pollutants in spaces, with an emphasis on tall spaces in which stratification can be assumed. For that purpose, a naturally ventilated sports hall is chosen as an example of a large enclosure with a high ceiling, in which the characteristics of the layer of stale air is to be investigated. Since computational fluid dynamics (CFD) has been proved to be a powerful tool for predicting airflow, commercial CFD simulation software is used to conduct a parametric analysis in order to determine the most influential factors on the dimensions of the stale air layer.

STATE–OF–THE–ART OF DISPLACEMENT VENTILATION

A major challenge for building designers is the supply of indoor air of sufficient quality. Two main principles prevail to meet this requirement, namely mixing ventilation and displacement ventilation. The philosophy of mixing ventilation is to provide fresh air via high velocity supply air streams in order to achieve fully mixed conditions in the space due to turbulence caused by the jets. It is therefore aspired to achieve a constant temperature and pollutant concentration profile. In other words, mixing type ventilation systems aim for air conditions in the extract flow, with regard to contaminant concentrations, to be an indication for the space as a whole. This is achieved by diluting the stale air as much as necessary to meet this condition (STYMNE et al., 1991).

The opposite applies to displacement ventilation. The main idea here is to allow warm contaminated air to rise towards the ceiling in thermal plumes generated by heat sources and extract it at high level. Cool fresh air on the other hand is supplied at low level with low velocity and is expected to spread out above the floor. For this purpose common displacement ventilation systems consist of special air diffusers. However, this strategy is also applicable to natural ventilation as it takes advantage of the stack effect which occurs due to the location of the supply and extract at low and high levels (LI, 2007). Thereby, the aim is to achieve supply air conditions in the occupants' breathing zone due to stratification of stale air at high level and fresh air at low level.

Spaces ventilated in this manner exhibit three regions with different flow patterns (SKISTAD et al., 2002). A uni–directional flow can be found in the lower zone followed by an interface with horizontal flow only. The upper–most zone is characterised by recirculation and is therefore called the recirculating region. As shown in figure 1, great importance is attached to the height of the interface, referred to as the neutral height z_n, because the contaminant concentration increases within this region to reach a relatively stable value in the upper zone.

Analytical models to determine the neutral height z_n exist for basic geometries and for simplified assumptions of the heat and contaminant sources (ETHERIDGE and SANDBERG, 1996; AWBI, 2003; MUNDT, 1995; LI, 2007). Theoretically, the neutral height is reached at a level where the sum of the plume

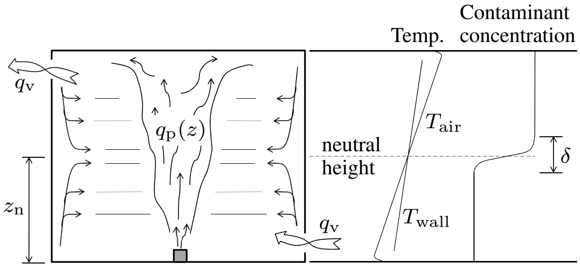

Figure 1: Principle of displacement ventialtion with temperature and contaminant concentration profiles (STYMNE et al., 1991)

flow rates $q_p(z)$ above heat sources equals the ventilation flow rate q_v. It can be found from measurements since it corresponds to the height at which the air temperature and the wall surface temperature are equal, as shown in figure 1 (AWBI, 2003). It is not to be confused with the neutral pressure level found in buoyancy driven natural ventilated spaces LINDEN et al. (1990).

A derivation of the maximum contaminant concentration x_{max} in the upper zone is possible with a balance between the contaminant production rate $\dot{M}$ and the mass lost due to ventilation from the extract (ETHERIDGE and SANDBERG, 1996). In this model the contaminant concentration does not exceed

$$x_{max} = \frac{\dot{M}}{q_v} \quad (1)$$

under steady state conditions. It is widely accepted that the interface thickness on the other hand is controlled by a balance between convection and diffusion (STYMNE et al., 1991) and that diffusion is the cause for the gradual increase in the concentration of contaminants. With the diffusion coefficient D_{AB} and the gradient of the plume flow rate the interface thickness can be obtained from

$$\delta = 2.5 \cdot \sqrt{\frac{D_{AB} \cdot A}{\frac{dq_p}{dz}}} \quad (2)$$

where A is the floor area (ETHERIDGE and SANDBERG, 1996). SI–units need to be used for the parameters here. Work on salt bath experiments confirms the influence of diffusion (KAYE et al., 2010). It is also known that the role of diffusion is even greater in ventilated rooms compared to salt bath modelling experiments.

SIMULATION METHODS

Understanding the contaminant concentration profile and its determining parameters is essential for designing a ventilation system. High rooms are often suitable for natural ventilation because of a stack driven airflow in the absence of wind when a difference in height between openings can be established. Therefore, the subject of this study is a sports hall located in Sontheim,

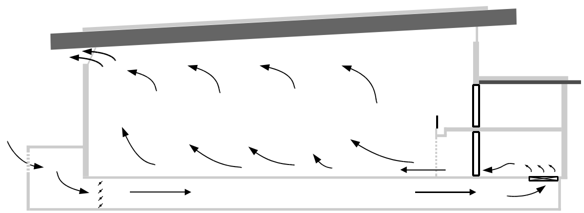

Figure 2: Sketch of ventilation strategy of the sports hall in Sontheim (HÖFKER and BÜCKLE, 2000)

Figure 3: Picture of the sports hall in Sontheim giving an overview of the geometry

near Stuttgart, Germany. It serves as a typical representation of high roofed rooms. The hall was built in 2001. As part of a natural ventilation strategy the hall comes with two subterranean concrete channels acting as a ground–to–air heat exchanger. Aiming for preheating the air in the winter and cooling the air in the summer, both channels running across the whole width of the hall. They end in tool sheds, where the air inlets are covered with gratings. As illustrated in figure 2, additional sliding heat exchangers are positioned at the inlets to further heat the inflowing air on cold days. Fresh air entering the main hall through the permeable sliding gates of the tool shed is intended to disperse across the floor and rise due to thermal plumes produced by the occupants. Finally, stale air leaves the hall through automatically controlled window sashes at high level. The sashes' opening sizes are regulated by two carbon dioxide sensors placed at head height at each of the shorter external walls. It is either possible to use the hall as a whole or divide it into two sections via a movable partition panel. In order to get an impression of the space a picture taken from inside is illustrated in figure 3.

The net sports area of the hall is made up of a rectangular zone with a size of about 44 m × 22 m. Since the partition panel is located in the middle, it is possible to divide this area into two squares equipped with one ventilation system each. Therefore, an additional

8 m in width provides space for two tool sheds with a length of about 15 m each. The roof is slightly sloped so that the height of the hall increases by about 1 m over the hall's width, starting from 8.5 m. The air supply duct's clear opening is 1.00 m × 1.80 m. An outside closing device is made from rotatable lamellas controlled by the same mechanism as the window sashes. The north orientated façade opposite the tool sheds is equipped with sixteen windows. All windows have a height of 1.30 m and are 1.40 m wide. They are arranged in two rows with their centres at a height of 3.45 m and 7.25 m above the floor. However, the lower row as well as eight smaller windows in the opposite façade located above the tool sheds only exist to meet the requirements of the fire protection strategy and are not used as part of the ventilation system.

The ventilation is controlled by two CO_2 sensors, as mentioned before. Lamellas in front of the air supply duct and the window sashes open at a concentration of 800 ppm. Initially, they do not open fully, but the opening size increases continuously with rising CO_2 concentration. That is to prevent unnecessarily high ventilation rates on cold days. However, in addition to the CO_2 the ambient temperature is another control parameter within this system. If it exceeds 15 °C, all windows and the air supply channel open to use pressure induced flow due to density differences as well as wind if available. If the ambient temperature falls below 15 °C, only the top row of the windows in the north façade open in combination with the openings in the supply channels. At the same time the heat exchanger heats the air at the inlet if required. In this process the heat exchanger's power output is controlled thermostatically. This ventilation system is designed to provide an amount of fresh air equal to 14 l/(s pers) for a total of 120 people.

Modelling the air flow in the sports hall in Sontheim with CFD is limited to one half of the hall, thought of as divided by the partition panel. The flow domain therefore covers a space of 22.15 m × 30.30 m with a height of 11.30 m. Here the first 1.8 m of height is exclusively used to accommodate the supply channel. Blockages fill the whole ground, so that the channel is left free with a width of 1.00 m, covered by a plate without thickness which represents the hall's floor. All unconnected spaces, such as dressing rooms, stair cases or plant rooms, are excluded from the flow domain by using blockages. The tool shed, however, is shaped by thin plates which are arranged in a manner to form two holes in the gates. Only ventilation due to buoyancy is considered in this research. To this end, all windows except the top row in the north oriented façade are neglected and not implemented in the CFD model. People taking exercise in the hall are simplified in the model to their most essential features. They are built out of cuboids, 1.5 m high having a ground area of 0.30 m × 0.30 m. In order to be able to imitate the contaminated exhalation, an inlet has been placed

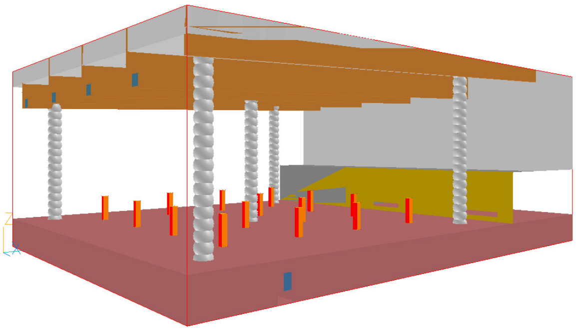

Figure 4: Overview of the geometry of the sports hall in Sontheim implemented in the CFD code showing the occupants as well as reading points used for the analysis

at the top of each cuboid taking up its whole area. This is to avoid additional geometrical discontinuities with respect to the computational grid resulting from a potentially smaller mouth. An image of the generated geometry is illustrated in figure 4. The additional heat exchanger at the outlet of the supply channel is neglected throughout all simulations.

Windows in the north oriented façade as well as the inlet at the supply channel are modelled with an orifice equation assuming a quadratic relationship between the flow rate and the pressure difference at the openings with a discharge coefficient of 0.61. Instead of a predetermined mass or volume flow through the openings, the flow velocity is deduced from the pressure differences occurring throughout the computation. The ventilation system is demand controlled and opening sizes vary corresponding to the indoor air quality. Due to the fact that simulations are run in steady state mode no regard is made to this effect. However, in order to take account of a reduced window area in reality the opening's areas are scaled down while the original aspect ratio is preserved and the centre of each opening remains at the same position.

A person's mouth is declared as inlet objects with a given volume flow rate. An appropriate flow rate is chosen in accordance to the respiratory minute volume RMV depending on the persons' physical activity. Thereby, the temperature of exhaled air and the CO_2 concentration are left unchanged at 33 °C (HÖPPE, 1981) and at 0.04 kg/kg (GUYTON and HALL, 2006), respectively. Turbulence intensity at the inlets is always at a value of 5.0%.

People's heat output is considered as fixed heat fluxes at the surfaces of the cuboids. All five surfaces turning towards the flow domain are equipped with the same heat load, although the top surface is considerably smaller than the others. Sixteen people are considered practicing table tennis at eight tables. This arrangement leads to a more or less even distribution of people on the sports area as depicted in figure 4.

The ambient air temperature is set to 18 °C, which is also the target temperature on cold days where the ambient air needs to be heated by the heat exchanger. Therefore, walls of the supply channel are considered to be adiabatic. While the total heat flux from the occupants is $\dot{Q} = 300$ W/pers, their respiratory minute volume amounts to $RMV = 40$ l/(min pers). The size of the windows is reduced to 16% of the actual opening size in order to take account of the demand controlled ventilation strategy.

Simulations of the flow in the sports hall are carried out in steady state mode. Thus, movement or physical activity of the occupants is neglected. This, however, is especially important in a sports hall where intense physical activity prevails and its effects on the distribution of CO_2 could be significant. Other CFD studies have revealed that moving objects can carry a contaminant in their wake, and that movement can cause a swing in the contaminant concentration at breathing level (MAZDUMAR et al., 2010). Nonetheless, a rather high level of physical activity is required to entirely abolish the displacement effect (MATTSSON, 1999). On the other hand, the displacement flow pattern is re–established fairly quickly after the activity is ceased (MAZDUMAR et al., 2010). As the occupant's movements in the sports hall are substantial the majority of the time, corresponding with their exercise, the disregard of movement appears to be one of the major weaknesses of the CFD model presented in this work.

In spite of that, steady state simulations are judged as sufficient to examine the global contaminant distribution pattern instead of the small scale flow features around people. Reynolds–Averaged Navier–Stokes equations are solved for finite volume elements to predict the fluid flow. Thereby, the high Reynolds number approximation of the RNG k–ϵ model (YAKHOT and ORSZAG, 1986) is used since it has been proven in the literature to be one the most promising turbulence models in predicting contaminant distribution in enclosed environments (ZHAI et al., 2007; ZHANG et al., 2007). Good results have been obtained with the model in studies on the air distribution in large spaces (SEKHAR and WILLEM, 2004) and the plume flow above heat sources (CRAVEN and SETTLES, 2006). The log–law function is used as the near wall treatment.

In order to study the distribution of an additional chemical species an extra variable is introduced in the CFD model. Both air as the main fluid and the additional chemical species representing CO_2 are treated identically as air at 20 °C and normal atmospheric pressure. All material properties are considered to be constant with a density of $\rho = 1.189$ kg/m^3, a laminar kinematic viscosity $\nu = 1.544 \cdot 10^{-5}$ m^2/s, a specific heat $c_P = 1005$ J/(kg K), a thermal conductivity $\lambda = 0.0258$ W/(m K) and a thermal expansion coefficient of $\beta = 0.00341$ 1/K. One advantage of taking the density of both constituents to be equal and constant is the possibility of making use of the Boussinesq approximation to model buoyancy effects. The initial concentration of CO_2 is set to 0.00038 for all grid points. It is also the CO_2 concentration of ambient air entering the flow domain through openings in the building envelope.

In order to enhance the solution algorithms the staggered grid approach has been applied to a structured mesh system in Cartesian coordinates. The solution strategy to resolve the problems associated with the non–linearities and the pressure–velocity linkage in the momentum equations used in this research is SIMPLEST. Convergence is controlled with the aid of a monitoring point near one of the outlets and the sums of the absolute residuals. Additionally, global source imbalances are checked for the continuity of mass, energy and contaminant concentration. In order to verify the outcome of the simulations analytical models are used for comparison of the ventilation flow rates, maximum CO_2 concentrations and mean internal air temperatures.

Due to a rather complicated flow field and the main focus of attention on the contaminant distribution in the space the prevailing problem is prone to artificial diffusion. Higher order differencing schemes should be used in order to achieve accurate solutions (VERSTEEG and MALALASEKERA, 2007). Therefore, higher order differencing schemes have been applied to solve the steady state airflow in the sports hall in Sontheim. However, convergence was not achieved for a variety of different differencing schemes. On this account a gradual grid refinement study was carried out using the HYBRID differencing scheme. Its formal order is problem dependent and not known in advance, because it switches between upwind differencing scheme UDS and central differencing scheme CDS as a function of the flow velocity. A monotonic grid refinement was conducted with three consecutive meshes as described by (ROACHE, 1997). The refinement factor of $r = 1.5$ was applied twice to all directions of the initial grid with $38 \times 36 \times 28$ grid cells. Therefore the middle grid counts $60 \times 54 \times 42$ and the fine grid $90 \times 81 \times 63$ nodes. As a target quantity, the species concentration of CO_2 was chosen. With the aid of an arbitrary monitoring point in the floor plan, a vertical contaminant profile is compared for all three different grids. These profiles are illustrated in figure 5. An estimation of the error inherent in each grid is given for CO_2 concentration at a height of 1.0 m. Absolute values of 852, 933 and 970 ppm at $z = 1.00$ m for the coarse, middle and fine grid respectively, have been used for the evaluation. While the order of the HYBRID differencing scheme can be found to be $p = 1.932$, the estimated error in the results decreases from 16.0% to 7.3% and 3.2% when the grid becomes finer. Finally, a trial on using the third order differencing scheme SMART (GASKELL and LAU, 1988) on the extra variable only and UDS for the remaining

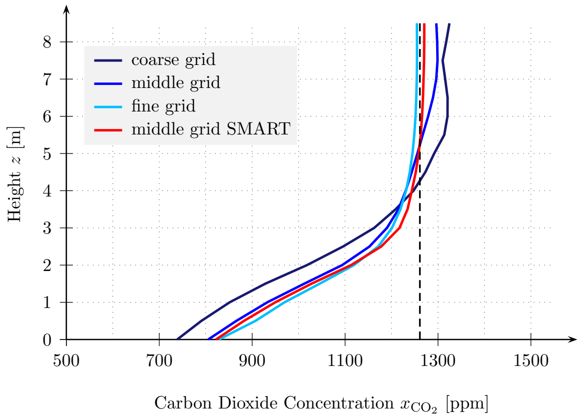

Figure 5: Results of grid refinement study, vertical CO_2 concentration profile in the sports hall for a reading point at $x = 2.00$ m and $y = 20.00$ m, the dashed lines represent the expected maximum

ones leads to a converged solution as well. This trial was carried out with the middle grid. Its CO_2 concentration profile approaches the one for the fine grid, with a slight offset, as can be seen in figure 5. An error cannot be calculated in the same manner as before because the order of the differencing scheme has changed. Nevertheless, figure 5 reveals that the error is likely to be less than 5%. In order to save computing time, this degree of accuracy is taken to be sufficient for a parametric study, as it is supposed to be smaller than the sum of all remaining errors and uncertainties in the model. As such, all the following simulations are carried out with a grid of $60 \times 54 \times 42$ cells and the differencing scheme SMART for the extra variable representing CO_2 and UDS for all others.

RESULTS

For the sake of a uniform presentation of the CFD results a system is established so that a comparison among different settings is possible. To this end, vertical profiles of the CO_2 concentration and the temperature are taken from the results at five reading points on the sports area of the hall for each case investigated. Four reading points are located in each corner 2.00 m away from the surrounding walls and one is placed in the centre between the heat and contaminant sources as depicted in figure 4. The average of all five reading points acts as the CO_2 concentration and temperature profile to be compared with the results of other simulations. It was observed that the distribution of CO_2 at each height was uniform, thus justifying the use of the average value over all monitoring points for comparison.

The first parameter varied is the heat generated by the occupants. In steps of 100 W/pers the total heat output is changed from 100 W/pers to 400 W/pers. The RMV as well as the heat output are dependent on physical activity. However, the RMV is left unchanged at a value of $RMV = 40$ l/(s pers). All surrounding surfaces are considered as adiabatic without any interaction due to radiation. As illustrated in figure 6 the CO_2 concentration rises gradually from the floor to a height of about 3.50 m where it reaches an almost constant value independent of the occupant's heat output. Black dashed lines in the diagram signify the expected maximum concentrations calculated with equation 1. The ventilation flow rate q_v required to carry out this computation is taken as the sum of the flow rates through the windows. While the lowest CO_2 concentration occurs for the highest rate of heat released from the people, the shape of the graphs is approximately the same with a horizontal translation only. The increment between the maximal concentrations increases with decreasing people's heat release. Temperature profiles are also similar to each other. However, highest temperatures as well as the largest temperature differences between the floor and the ceiling occur at the maximal total heat output and a maximal ventilation rate. The general shape of the graphs is more parabolic, with a slight variation in slope at the ground. Again, a fairly stable value is reached at approximately 3.50 m so that the temperature does not notably change at higher levels. Since the general temperature profile does not vary significantly throughout the simulations it is waived to present all temperature profiles here.

The effect of the position, or more precisely the height of the windows, on the distribution of the CO_2 concentration and the temperature is also analysed for the sports hall. The height of the existing windows, i.e. the distance from the floor to the opening's centre, is reduced in the CFD model from 7.00 m down to 2.50 m. Figure 7 shows the impact of a reduced window height on the vertical concentration profile. Due to a lower ventilation flow rate CO_2 concentration decrease with a reduction in the height of the windows. Estimations of the maximum concentration according to equation 1 become more uncertain with lower window heights.

As a next step, the properties of the surfaces are changed from adiabatic to a fixed surface temperature. This refers to surfaces of external walls only. The vitreous part of the north façade, for example, is given a constant temperature of 14 °C, and 19 °C is set on all concrete walls. This implies an ambient temperature of -5 °C and an internal temperature of about 20 °C with averaged U–values for transparent and opaque building elements at steady state conditions. All other surfaces are considered as adiabatic. However, the ambient temperature is left at $\vartheta_a = 18$ °C to represent the use of the heat exchanger at the end of the supply duct. Heat exchange with cold surface temperature has a striking impact on the distribution pattern of carbon dioxide, particularly at low levels, while the slope in the concentration profile remains almost unchanged, the height where the constant value is reached decreases remarkably, illustrated in figure 8. At a height of $z = 1.50$ m the carbon dioxide con-

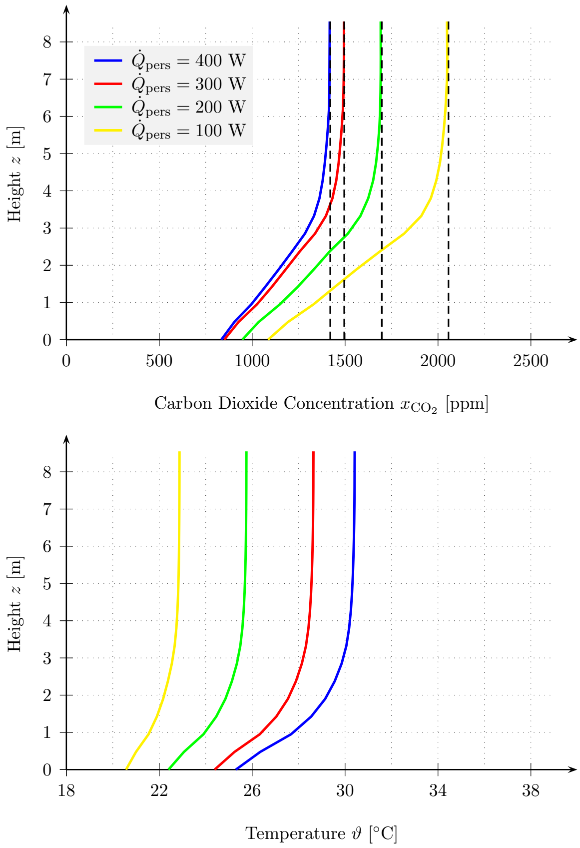

Figure 6: Vertical CO_2 concentration and temperature profiles for a variable heat output from the occupants with $\vartheta_a = 18$ °C, $RMV = 40$ l/(min pers), 16% of the original opening size and adiabatic surfaces

centration rises by approximately 350 ppm over that of adiabatic surfaces, giving an equivalent increase of more than 30%.

DISCUSSION OF THE SIMULATION RESULTS

Throughout all simulations the maximum CO_2 concentration predicted by equation 1 matches the simulated maximum concentration well, as depicted in figures 6 to 8. Larger deviations are observed for a reduced window height. This results in a decreased content of CO_2 in the exhaust. The simplified model to predict the maximum concentration works well. It is therefore applicable as a simple design tool to estimate the maximum concentration in larger enclosures with displacement ventilation. Due to its constraints the application should be limited to high spaces where the outlets are located near the ceiling height.

The first simulations of the parametric analysis presented were run with the surrounding surfaces modelled as adiabatic. Parameters varied throughout the simulations, such as heat output of the occupants or the height of the openings, should influence the general CO_2 distribution pattern in the space according the theory of displacement ventilation typified in figure 1. A distinct interface at which the CO_2 concentra-

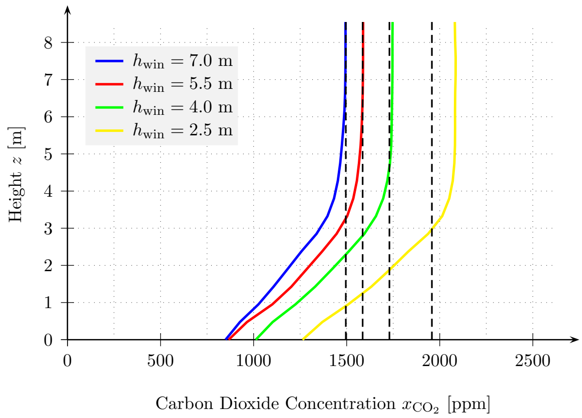

Figure 7: Vertical CO_2 concentration profile for a variable window height with $\vartheta_a = 18$ °C, $\dot{Q} = 300$ W/pers, $RMV = 40$ l/(min pers)and 16% of the original opening size

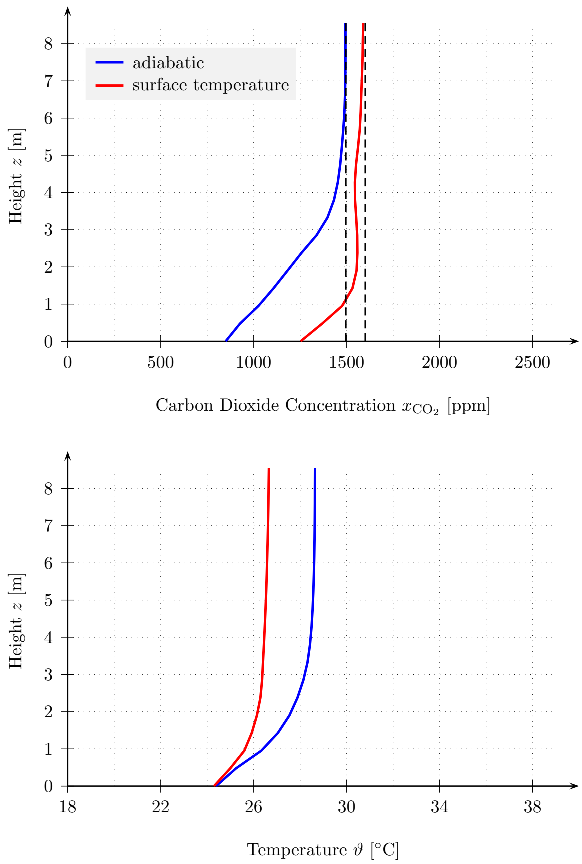

Figure 8: Vertical CO_2 concentration and temperature profiles for a fixed surface temperature at selected surfaces with $\vartheta_a = 18$ °C, $\dot{Q} = 300$ W/pers and $RMV = 40$ l/(min pers)

tion undergoes a sharp increase, with the regions above and below the interface exhibiting higher and lower carbon dioxide concentrations, respectively, does not exist in these simulation results. However, in figures 6 and 7 a rising CO_2 concentration from the floor to a height of about $z = 3.50$ m, whereupon the concentration remains constant, can be observed in all cases investigated.

The plume flow rate in this thermally stratified surrounding can be modelled analytically (MUNDT, 1995). Assuming the temperature gradient to be constant it can be shown that the plume flow rate already exceeds the ventilation flow rate at floor height in all cases. Therefore, the neutral height is assumed to be at $z = 0.0$ m.

If the graphs representing the distribution of carbon dioxide in figures 6 and 7 are extended to negative values, they all end at a common point of intersection for the cases of varying heat output of the occupants and varying window height. This point is located at a concentration of 380 ppm, which is equivalent to the CO_2 content of clean air.

Furthermore, an estimation of the interface thickness is possible by using equation 2. While the floor area of the hall is given by the geometry, the gradient $\mathrm{d}q_\mathrm{p}/\mathrm{d}z$ at floor height is taken from the analytical model, whereas the diffusion coefficient D_AB can be obtained from the results of the CFD simulations. Due to the large floor area and a high turbulent diffusion coefficient an interface thickness of approximately $\delta = 4.00$ m could be expected in the present case. This large interface thickness causes the air quality in the breathing zone to be better compared to higher levels even in the absence of a typical contaminant concentration profile for displacement ventilation.

The general CO_2 distribution pattern does not change although parameters influencing the plume flow rate and the ventilation flow rate have been altered. On the other hand, the surface temperature seems to be the crucial parameter that changes the distribution pattern. Figure 8 demonstrates that additional vertical air flows caused by cold downdrafts from the wall transport contaminated air from higher to lower levels and thereby increase the CO_2 concentration in the breathing zone. Furthermore, the maximum concentration increases with decreasing air temperature due to a reduced flow rate caused by smaller temperature differences between the ambient and internal air. Lower indoor temperatures allow for a greater maximum concentration of contaminant in the slower moving and less ventilated air. Therefore it is advisable to increase the quality of the building's envelope, i.e. the thermal insulation, so that the desirable air quality with respect to CO_2 concentration can be achieved without increasing the ventilation flow rate. However, it should be kept in mind that the surface temperature depends on other factors such as solar irradiation, thermal admittance of the building material and internal heat gains. It is a highly transient quantity, particularly in the present case of the sports hall where intermittent occupancy prevails.

The parametric analysis itself showed that the thermal properties i.e. the heat loss, or more precisely the surrounding surface temperatures , are of primary importance in the distribution of CO_2. It is therefore generally advisable to thoroughly determine the actual boundary conditions if an accurate prediction of absolute values is desired. If surface temperatures are measured directly in order to serve as boundary conditions for a CFD model this data already contains radiation. Otherwise the radiation between the surroundings should be considered in any simulation as its influence on the contaminant distribution might be significant. Special attention should be paid when defining boundary conditions if indoor environments are enclosed by transparent building elements through which solar irradiation is transmitted to internal surfaces.

CONCLUSIONS

A numerical study on the carbon dioxide distribution has been conducted using the example of a naturally ventilated sports hall, representing large and high enclosures. Equipped with an inlet at low–level and several outlets at high–level the space has been designed to be ventilated by displacement ventilation induced by buoyancy forces from internal heat sources. Parameters influencing the CO_2 distribution according to the theory of displacement ventilation have been examined aiming for a better understanding of the contaminant distribution in large spaces.

A distinct vertical concentration profile as predicted from the theory of displacement ventilation, with a lower region of fresh air and an upper contaminated region, separated by an interface at which the CO_2 concentration sharply increases, could not be found in any of the cases studied. The height of this interface instead turned out to be at floor level. However, due to the large thickness of the interface a stratification of contaminants with better air quality in the breathing zone can be achieved.

Additional vertical airflow induced by temperature differences between the internal air and the surrounding surfaces contribute remarkably to the CO_2 distribution in the space. In fact, during this research surface temperatures turned out to be one of the most important factors in the study of contaminant distribution. Cold downdraughts are likely to carry contaminated air from the upper layer down to the occupant's breathing zone with striking impact on air quality. Moreover, it has been revealed that the maximum contaminant concentration in a room is reasonably well predictable if exhaust openings are at high level, i.e. where the concentration has reached its maximum.

Nevertheless, CFD has been shown to be a powerful tool for the analysis of airflow and related topics in this research and might be one way to further investigate the problems which have emerged during this study. CFD is well suited for additional work on the variation of the interface thickness with varying floor areas, since changes in the geometry are easy to implement. Further work is also needed on the effect of surface temperatures on contaminant distribution in spaces. Also of interest is the impact of different ratios between the surrounding surfaces and the volume of the room on the nature of displacement ventilation with respect to their surface temperatures, since most work presented in the literature is limited to small test rooms having a simple geometry.

ACKNOWLEDGEMENT

This work has been sponsored by the German Federal Ministry of Education and Research (BMBF), which is here gratefully acknowledged. The promotional reference is 17032X10.

References

Building Bulletin 101. 2006. *Ventilation of School Buildings*. Regulations, Standards, Design Guidance, Version 1.4.

AWBI, H. B. 2003. *Ventilation of Buildings*. Taylor & Francis Group, London, New York, second edition.

CRAVEN, B. A. and SETTLES, G. S. 2006. A computational and experimental investigation of the human thermal plume. *Journal of Fluids Engineering*, 128(6):1251–1258.

ETHERIDGE, D. and SANDBERG, M. 1996. *Building Ventilation: Theory and Measurement*. John Wiley & Sons, Inc., Chichester, New York.

GASKELL, P. H. and LAU, A. K. C. 1988. Curvature-compensated convective transport: SMART, a new boundedness- preserving transport algorithm. *Numerical Methods in Fluids*, 8(6):617–641.

GUYTON, A. C. and HALL, J. E. 2006. *Textbook of Medical Physiology*. Elsevier Saunders, Philadelphia, eleventh edition.

HÖFKER, G. and BÜCKLE, A. 2000. *Natürliche Belüftung – Sporthalle des TSV 1892 HN–Sontheim e.V.* Technical report of engineering consultants, Backnang.

HÖPPE, P. 1981. Temperatures of expired air under varying climatic conditions. *International Journal of Biometeorology*, 25(2):127–132.

KAYE, N. B., FLYNN, M. R., COOK, M. J., and JI, Y. 2010. The role of diffusion on the interface thickness in a ventilated filling box. *Journal of Fluid Mechanics*, 652:195–205.

LI, Y. 2007. Bouyancy–driven natural ventilation in a thermally stratified one–zone building. *Building and Environment*, 35:207–214.

LINDEN, P. F., LANE–SERFF, G. F., and SMEED, D. A. 1990. Emptiying filling boxes: the fluid mechanics of natural ventilation. *Journal of Fluid Mechanics*, 212:309–335.

MATTSSON, M. 1999. *On the Efficiency of Displacement Ventilation, with particular Reference to the Influence of Human Physical Activity*. PhD thesis, University of Gävle.

MAZDUMAR, S., YIN, Y., GUITY, A., MARMION, P., GULICK, B., and CHEN, Q. 2010. Impact of moving objects on the contaminant concentration in an inpatient ward with displacement ventilation. *HVAC&Research*, 16(5):545–564.

MUNDT, E. 1995. Displacement ventilation systems – convection flows and temperature gradients. *Building and Environment*, 30(1):129–133.

ROACHE, P. J. 1997. Quantification of uncertainty in computational fluid dynamics. *Annual Review of Fluid Mechanics*, 29:123–160.

SEKHAR, S. C. and WILLEM, H. C. 2004. Impact of airflow profile on indoor air quality - a tropical study. *Building and Environment*, 39:255–266.

SKISTAD, H., MUNDT, E., NIELSEN, P. V., HAGSTRÖM, K., and RAILIO, J. 2002. *Displacement ventilation – in non–industrial premises*. Rehva, Brussels.

STYMNE, H., SANDBERG, M., and MATTSON, M. 1991. Dispersion pattern of contaminants in a displacement ventilated room – implications for demand control. Air Movement & Ventilation Control within Buildings, 12th AIVC Conference, pages 173–189, Ottawa, Canada.

VERSTEEG, H. K. and MALALASEKERA, W. 2007. *An Introduction to Computational Fluid Dynamics - The Finite Volume Method*. Pearson, Harlow, second edition.

YAKHOT, V. and ORSZAG, S. A. 1986. Renormalization group analysis of turbulence. I basic theory. *Journal of Scientific Computing*, 1(1):3–51.

ZHAI, Z., ZHANG, Z., ZHAN, W., and CHEN, Q. 2007. Evaluation of various turbulence models in predicting airflow and turbulence in enclosed environments by CFD part-1: Summary of prevalent turbulence models. *HVAC & R Research*, 13(6):853–870.

ZHANG, Z., ZHAN, W., ZHAI, Z., and CHEN, Q. 2007. Evaluation of various turbulence models in predicting airflow and turbulence in enclosed environments by CFD part-2: Comparison with experimental data from literature. *HVAC & R Research*, 13(6):871–886.